Stationary properties of high-T_c Josephson structures with a noble metal layer

A. A. Golubov and M. Yu. Kupriyanov

Scientific-Research Institute of Nuclear Physics, 112863 Moscow, Russia
(Submitted 24 December 1993)
Zh. Eksp. Teor. Fiz. **105**, 1442–1455 (May 1994)

The stationary properties of SNS Josephson junctions with SN boundaries of small transparency have been investigated in the framework of the microscopic theory of superconductivity. It has been assumed that the suppression of superconductivity in the electrodes resulting from the proximity effect is negligibly small, that the conditions in the "dirty" limit are satisfied in the normal metal, and that the junction is quasi-one-dimensional. Analytical expressions have been obtained for the temperature dependence of the critical current of a junction J_c with an arbitrary relationship between γ_{B1} and γ_{B2} in the range of small thicknesses of the N layer ($d \ll \xi_n^*$) over the entire range of temperatures, as well as for arbitrary d and $T \gg T_c/[\gamma_{B1}\gamma_{B2}/(\gamma_{B1}+\gamma_{B2})\min\{1,d/\xi_n^*\}]$. The analytical expression for $J_c(T)$ obtained for symmetric structures ($\gamma_{B1}=\gamma_{B2}$) holds at arbitrary values of T and d. It has been shown that J_c for asymmetric structures differs from J_c for symmetric structures by no more than twofold. The results of the calculations are in satisfactory agreement with the existing experimental data. It has been shown that the disparity between the spatial distributions of the normal current and the supercurrent in the structures gives rise to a resistance shunting the junction and additional suppression of the J_cR_n product. The additional suppression of J_cR_n due to the mutual character of the proximity effect in the N material of the structures has also been evaluated.

1. INTRODUCTION

The analysis in Ref. 1 showed that as a consequence of the high chemical activity of high-T_c superconducting materials, only noble metals (Ag, Au) can serve as the material of the normal metal layer in high-T_c SNS Josephson structures. So far, two types of such junctions have been created experimentally: planar SNS structures[2–4] and step-edge junctions.[5–13] The interest in studying the processes occurring in these structures is attributable both to the achievement of high values of the product $J_cR_n \approx 10$ mV ($T=4.2$ K) and 1 mV ($T=77$ K) in them[11] and to the possibility revealed for studying the properties of high-T_c superconductor/Ag, Au boundaries, which have small transparencies. It is noteworthy that there is a whole class of low-T_c Josephson junctions with semiconducting layers having similar properties.[14]

The first stage of the technology for fabricating planar structures calls for the *in situ* sputter-deposition of a two-layer structure consisting of a high-T_c superconducting film grown epitaxially on a substrate (generally $SrTiO_3$) (with the C axis perpendicular to the substrate) and a cover of silver or gold.[2,3] Then the SN sandwich created is cut in two by photoelectron lithography or by means of a high-energy ion beam to form two composite SN electrodes separated by a gap $L \approx 0.1$–0.2 μm. An Ag or Au film, which links the two electrodes, is sputter-deposited in the final stage to form a Josephson structure, and its width is fixed.

The fabrication of step-edge junctions is begun by etching a sharp step with a height of 150–250 nm in a substrate ($SrTiO_3$, $LaAlO_3$, $NdGaO_3$). Then C-axis oriented high-T_c superconducting electrodes having a thickness (50–150 nm) that ensures the absence of electrical contact between them in the step region are deposited by angled sputtering. Afterwards, a silver film, which links these electrodes, is deposited *in situ* in the same chamber. The process is completed by imparting the required geometric dimensions to the junction by ordinary photolithographic methods.

In both cases the geometric dimensions of the weak-link region $d \approx 50$–10 nm are of the order of the coherence length of the normal metal $\xi_n^* = (D/2\pi T_c)^{1/2} \approx 30$ nm, where D is the diffusion coefficient and T_c is the critical temperature of the high-T_c superconducting electrodes. This range of values exceeds the range of applicability of the existing theoretical models,[1] which describe the properties of high-T_c SNS structures only for small ($d \ll \xi_n^*$) or large $d/\xi_n^* \gg (T_c/T)$ distances between the electrodes. In addition, the presence of several boundaries with significantly different transparencies in the structures also imparts essentially specific details to their behavior, causing differences in the spatial distributions of the normal current and supercurrent, which, as will be shown below, must be taken into account in evaluating the characteristic voltages of the junctions.

In this study we derived an analytical expression for the temperature dependence of the critical current I_c of planar structures, which is valid for an arbitrary relationship between d and ξ_n^*, analyzed the influence of the geometric features and boundaries of different transparency on the parameters of Josephson junctions, and determined the main factors which result in the suppression of J_cR_n in high-T_c SNS structures.

 1063-7761/94/050777-08$10.00

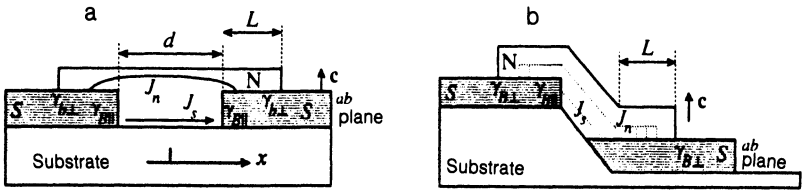

FIG. 1. Schematic representations of planar (a) and step-edge (b) SNS Josephson structures.

2. MODEL OF AN SNS JUNCTION

We assume that the dimensions of a junction in its plane are small compared with the Josephson penetration depth, that the conditions of the "dirty" limit are satisfied in the weak-link material, and that the parameters $\gamma_{B\perp}$ and $\gamma_{B\parallel}$, which characterize the transparency of each boundary, satisfy the inequalities:

$$\gamma_{B\perp}=\frac{R_{B\perp}}{\rho_n\xi_n^*}\gg\max\left\{1,\gamma_\perp=\frac{\rho_\perp\xi_\perp^*}{\rho_n\xi_n^*}\right\}, \tag{1a}$$

$$\gamma_{B\parallel}=\frac{R_{B\parallel}}{\rho_n\xi_n^*}\gg\max\left\{1,\gamma_\parallel=\frac{\rho_\parallel\xi_\parallel^*}{\rho_n\xi_n^*}\right\}. \tag{1b}$$

Here $R_{B\perp}$, $R_{B\parallel}$, $\rho_\perp$, and $\rho_\parallel$ are the resistivities of the SN boundaries and the S materials; $\xi_\perp^*$ and $\xi_\parallel^*$ are the coherence lengths when the c axis is perpendicular and parallel to the planes of these boundaries, respectively; ρ_n and ξ_n^* are the resistivity and coherence length of the normal metal. The validity of these inequalities at boundaries between high-T_c superconductors and noble metals follows both from the body of experimental facts[1] and from theoretical evaluations.[14-17]

The absence of a microscopic theory of high-temperature superconductivity precludes the performance of rigorous calculations that take into account the spatial variations in the superconducting properties of the electrodes near the SN boundaries. However, it was previously shown during an analysis of the proximity effect in the BCS approximation[18] β that these variations are negligibly small in the range of values of parameters (1) of interest to us. Moreover, the experimental temperature dependences of the order parameter $\Delta(T)/\Delta(0)$ in spatially uniform high-T_c superconducting materials are close to the dependence following from the BCS approximation. These circumstances permit the assumption that the order parameter in the S electrodes is constant and equal to $\Delta(T)$, which reduces the problem to solving the Usadel equations[19] in the N layer. The latter may be written in a calibration with a zero vector potential in the form

$$\Phi=\xi_n^{*2}\frac{\pi T_c}{\omega G}\nabla[G^2\nabla\Phi],\quad G=\frac{\omega}{\sqrt{\omega^2+\Phi^*\Phi}}, \tag{2a}$$

$$J=2\pi T_c\rho_n^{-1}\,\mathrm{Im}\sum_\omega\omega^{-2}G^2\Phi^*\nabla\Phi. \tag{2b}$$

Here $\omega=\pi T(2n+1)$ denotes the Matsubara frequencies, J is the supercurrent density, and ∇ is a two-dimensional differential operator.

System of equations (2) must be supplemented by boundary conditions at the interfaces between the S and N materials[18]

$$\gamma_B\xi_n^*G\nabla_n\Phi=G_s[\Delta\exp(\pm i\varphi/2)-\Phi],\quad G_s=\frac{\omega}{\sqrt{\omega^2+\Delta^2}}, \tag{2c}$$

in which φ is the phase difference between the order parameters of the electrodes, $\gamma_B=R_B/\rho_n\xi_n^*$ is a parameter determined by the experimental value of the resistivity of the SN boundaries R_B, ∇_n is the derivative with respect to a normal to the boundary, and Δ is the absolute value of the order parameter.

3. CRITICAL CURRENT OF AN SNS JUNCTION

The typical geometry of a planar SNS structure is presented in Fig. 1a. The significant difference between the transparencies of the SN boundaries in the directions parallel and perpendicular to the crystallographic c axis permits neglect of the supercurrent flowing in the regions of

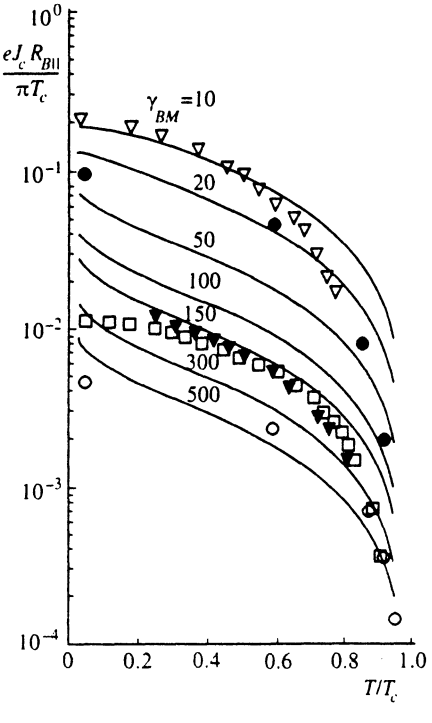

FIG. 2. Temperature dependence of the critical current of symmetric SNS structures ($\gamma_{B1}=\gamma_{B2}=\gamma_B$) calculated in the limit of small N-layer thicknesses at fixed values of the suppression parameter $\gamma_{BM}=\gamma_B d/\xi_n^*$. The points represent experimental data from Refs. 3 (▽, ▼), 5 (●), 9 (□), and 6 (○).

the normal metal lying on the electrodes, which, as the calculations in Ref. 20 showed, is $\gamma_{B\|}/\gamma_{B\perp}$ times smaller than the critical value. This situation greatly simplifies the calculations of J_c, reducing them to solution of the one-dimensional problem in the normal metal located in the gap between the electrodes.

$$\Phi=\xi_n^{*2}\frac{\pi T_c}{\omega G}[G^2\Phi']', \tag{3}$$

$$\gamma_{B1,B2}\xi_n^*G\Phi'=G_s[\Delta\exp(\pm i\varphi/2)-\Phi], \quad X=\pm d/2. \tag{4}$$

Here the prime sign denotes differentiation with respect to x, which is measured from the middle of the N layer perpendicularly to the interfaces between the materials (see Fig. 1a). The solution of this problem is simplified in several limiting cases.

3.1. Approximation for small values of Φ

At temperatures near the critical temperature, as well as when the thickness of the N layer is not excessively small, equations and boundary conditions (3) and (4) are linearized ($G\approx 1$) by virtue of inequality (1) and have an analytic solution of the form

$$\Phi=A\cosh(\beta x)+B\sinh(\beta x), \quad \beta=\frac{1}{\xi_n^*}\sqrt{\frac{\omega}{\pi T_c}}$$

$$A=\frac{G_s}{\delta}\left[[(\Gamma_1+\Gamma_2)R_s+i(\Gamma_1-\Gamma_2)I_s]\cosh\left(\frac{\beta d}{2}\right)+2G_sR_s\sinh\left(\frac{\beta d}{2}\right)\right],$$

$$B=\frac{G_s}{\delta}\left[[i(\Gamma_1+\Gamma_2)I_s+(\Gamma_1-\Gamma_2)R_s]\sinh\left(\frac{\beta d}{2}\right)+2iG_sI_s\cosh\left(\frac{\beta d}{2}\right)\right], \tag{5}$$

$$\delta=(G_s^2+\Gamma_1\Gamma_2)\sinh\left(\frac{\beta d}{2}\right)+(\Gamma_1+\Gamma_2)G_s\cosh\left(\frac{\beta d}{2}\right),$$

$$\Gamma_{1,2}=\beta\xi_n^*\gamma_{B1,B2},$$

in which $R_s=\Delta\cos(\varphi/2)$ and $I_s=\Delta\sin(\varphi/2)$ are the real and imaginary parts of the order parameter of the electrodes and i is imaginary unity.

The substitution of solution (5) into expression (2b) for the supercurrent gives a sinusoidal dependence of $J(\varphi)$ with a critical current density J_c equal to

$$J_c=\frac{4\pi T}{e\rho_n\xi_n^*(\gamma_{B1}+\gamma_{B2})}\times\sum_\omega\frac{\Delta^2}{(\omega^2+\Delta^2)[\Gamma_{\text{eff}}\sinh(\beta d)+G_s\cosh(\beta d)]}, \tag{6}$$

$$\Gamma_{\text{eff}}=\sqrt{\frac{\omega}{\pi T_c}}\gamma_{\text{eff}}, \quad \gamma_{\text{eff}}=\frac{\gamma_{B1}\gamma_{B2}}{(\gamma_{B1}+\gamma_{B2})}.$$

The expression for J_c holds provided there is fulfillment of the inequality

$$\Delta\ll\omega\frac{\gamma_{\text{eff}}\sinh(\beta d)+\cosh(\beta d)}{\cosh(\beta d/2)}, \tag{7}$$

which is violated at temperatures $T\ll T_c/(\gamma_{\text{eff}}\min\{1,d/\xi_n^*\})$. This range is larger, the smaller is the thickness of the N layer d as compared with ξ_n^*. Therefore, the region of small values of d should be treated separately.

3.2. Approximation for small N-layer thicknesses

When the thickness of the N layer is small, a solution of Eqs. (3) can be sought in the form of a series in d/ξ_n^*:

$$\Phi=A+B\frac{x}{\xi_n^*}+A\frac{\omega}{2\pi T_cG}\left[\frac{x}{\xi_n^*}\right]^2. \tag{8}$$

It is not difficult to obtain the following expressions for the constants A and B appearing in (8) from boundary conditions (4):

$$A=\frac{\Delta\gamma_{B1}+\Delta\gamma^*_{B2}}{(\gamma_{B1}+\gamma_{B2})[1+(\gamma_{\text{eff}}d/\xi_n^*)\alpha]}, \quad \alpha=(\omega/\pi T_cG_s), \tag{9}$$

$$B=\frac{G_s}{G}\frac{\alpha(\Delta\gamma_{B1}-\Delta^*\gamma_{B2})d/2\xi_n^*+\Delta-\Delta^*}{(\gamma_{B1}+\gamma_{B2})[1+(\gamma_{\text{eff}}d/\xi_n^*)\alpha]}. \tag{10}$$

Substituting (8)–(10) into expression (2b) for the supercurrent, we arrive at the nonsinusoidal dependence of $J_s(\varphi)$

$$J_s=\frac{2\pi T}{e\rho_n\xi_n^*(\gamma_{B1}+\gamma_{B2})}\sum_\omega\frac{GG_s\Delta^2\sin(\varphi)}{\omega^2[1+(\gamma_{\text{eff}}d/\xi_n^*)\alpha]}, \tag{11a}$$

$$G=\frac{\omega[1+(\gamma_{\text{eff}}d/\xi_n^*)\alpha]}{\sqrt{\omega^2[1+(\gamma_{\text{eff}}d/\xi_n^*)\alpha]^2+\Delta^2[1-(4\gamma_{eff}/(\gamma_{B1}+\gamma_{B2})]\sin^2(\varphi/2)}}, \tag{11b}$$

When $\gamma_{B1}=\gamma_{B2}$, expression (11) takes the form previously established[18] for symmetric junctions. Plots of the dependence of J_sR_n calculated in this case from (11) are presented in Fig. 2. The points in this figure represent experimental data obtained for SNS junctions of various types. As will be shown below, the differences observed, especially at low temperatures, are attributable to the finite width of the normal metal layer, which generally did not satisfy the requirement $d\leqslant\xi_n^*$.

It is noteworthy that when the symmetry of the bound-

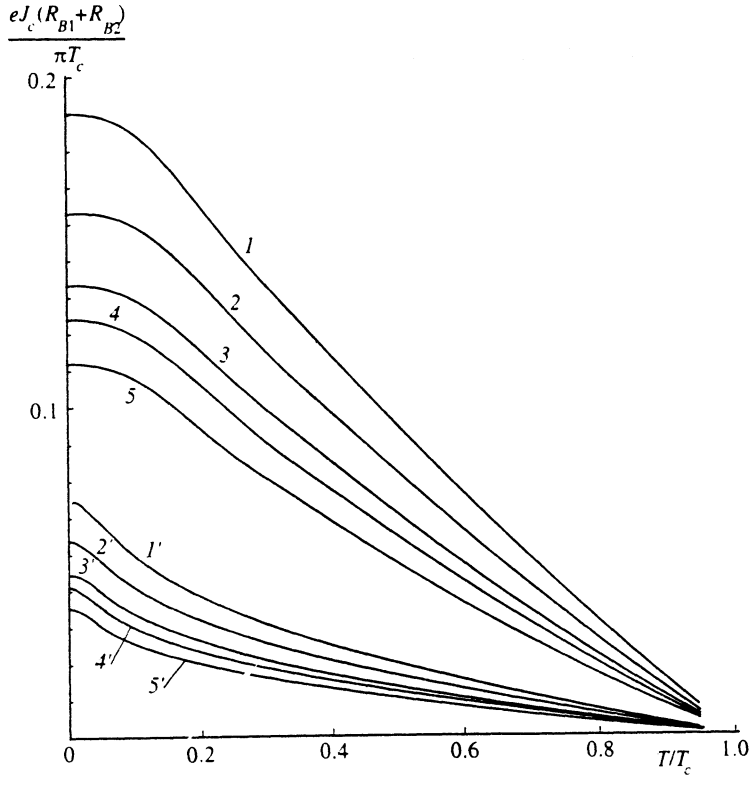

FIG. 3. Temperature dependence of the critical current of asymmetric SNS structures calculated in the limit of small N-layer thicknesses at fixed values of the suppression parameter $\gamma_{BM}=\gamma_B d/\xi_n^*=10$ (curves *1–5*), 50 (curves *1′–5′*) and various values of γ_{B1}/γ_{B2}: *1*, *1′*) 1; *2*, *2′*) 0.25; *3*, *3′*) 0.1; *4*, *4′*) 0.05; *5*, *5′*) 0.

ary transparencies is violated, $J_s(\varphi)$ as defined by (11a) deforms, tending to a sinusoidal function when $\gamma_{B2}\gg\gamma_{B1}$. However, as follows from the temperature dependences of J_sR_s calculated for various values of γ_{B1}/γ_{B2} (see Fig. 3), the absolute values of J_sR_n decrease by no more than two fold, reaching the known results for SNIS tunnel junctions in the limit $\gamma_{B2}\gg\gamma_{B1}$.[21] This fact is physically obvious. In symmetric structures the superconducting properties diffuse into the N region from the two electrodes, so that

$$\mathrm{Re}\Phi\propto\Delta/\gamma_{\mathrm{eff}}=\Delta(\gamma_{B1}^{-1}+\gamma_{B2}^{-1})\approx 2\Delta/\gamma_{B1}.$$

It is easily seen that in the limiting asymmetric case $\gamma_{B1}^{-1}\gg\gamma_{B2}^{-1}$, the latter term in the expression for Re Φ is small and Re Φ and, therefore, J_sR_n are approximately two times smaller than in symmetric structures T_0. The fact that J_sR_n does not depend on γ_{B2} is also obvious, since in this limit, as in ordinary tunnel junctions, $J_c\propto\gamma_{B2}^{-1}$, and $R_n\approx R_{B2}$.

3.3. Symmetric junctions ($\gamma_{B1}\approx\gamma_{B2}=\gamma_B$)

It follows from the structure of expressions (5), (9), and (10) that in approximation (1) of large values of γ_B, in which we are interested, the imaginary part of the Usadel functions in the N region is small at all temperatures

$$\mathrm{Im}\,\Phi\ll\sqrt{\omega^2+\mathrm{Re}\,\Phi^2} \tag{12}$$

and Eq. (3) has an analytic solution

$$\mathrm{Re}\,\Phi=\omega\frac{2\kappa\sqrt{(1-\kappa^2)}\,\mathrm{cn}(u)}{\mathrm{dn}^2(u)-2(1-k^2)},$$

$$\mathrm{Im}\,\Phi=A\,\mathrm{Re}\,\Phi\int_0^x\frac{dx}{G^2\,\mathrm{Re}\,\Phi^2}, \tag{13}$$

$$G=1-\frac{2(1-\kappa^2)}{\mathrm{dn}^2(u)},\quad u=\frac{x}{\xi_n^*}\sqrt{\frac{\omega}{\pi T_c}}, \tag{14}$$

in which $\mathrm{cn}(x)$ and $\mathrm{dn}(x)$ are Jacobi's elliptic functions, and the integration constants κ and A are determined from boundary conditions (4):

$$\kappa=\frac{\mathrm{dn}(q)}{\mathrm{cn}(q)}\sqrt{\frac{1}{2}+\frac{\Omega}{2\sqrt{\Omega^2+\mathrm{Re}\,\Phi_s^2}}},$$

$$A=\frac{\Omega\omega G_sR_sI_s}{\sqrt{\Omega^2+R_s^2}(\Omega+p\sqrt{\Omega^2+R_s^2}}$$

$$\Omega=\omega\left[1+\gamma_B\sqrt{\frac{\omega}{\pi T_c}}\frac{\mathrm{dn}(q)\mathrm{sn}(q)}{G_s\mathrm{cn}(q)}\right], \tag{15}$$

$$p=\frac{\mathrm{sn}(q)\mathrm{cn}(q)}{\mathrm{dn}^3(q)}\int_0^q\frac{\mathrm{dn}^4(u)}{\mathrm{cn}^2(u)}du,$$

$$q=\frac{d}{2\xi_n^*}\sqrt{\frac{\omega}{2\pi T_c}}.$$

The integration constants were essentially found by utilizing the useful relation between the values of the real parts of the Green's functions on the two sides of an SN boundary

$$\operatorname{Re}\Phi(d/2)=\operatorname{Re}\Phi_s\left[1+\gamma_B\sqrt{\frac{\omega}{2\pi T_c}}\frac{\operatorname{dn}(q)\operatorname{sn}(q)}{G_s\operatorname{cn}(q)}\right]^{-1}. \tag{16}$$

Substitution of the solution found into expression (2b) for the supercurrent gives a nonsinusoidal dependence of $J_s(\varphi)$:

$$J_s=\frac{2\pi T}{e\rho_n\xi_n^*\gamma_B}\sum_\omega\frac{\Delta^2\sin(\varphi)}{\sqrt{(\omega^2+\Delta^2)(\Omega^2+R_s^2)}}\times\frac{\Omega}{\Omega+p\sqrt{(\Omega^2+R_s^2)}}. \tag{17}$$

When the thickness of the normal metal layer is small ($d\ll\xi_n^*$), using the asymptotic expansions of the elliptic functions

$$\operatorname{sn}(u)=u-(1+\kappa^2)\frac{u^3}{6},\quad \operatorname{cn}(u)=1-\frac{u^2}{2},$$

$$\operatorname{dn}(u)=1-\frac{u^2\kappa^2}{2},$$

we can easily see that in (17) $p\approx q^2\propto(d/\xi_n^*)^2$ and that in a first approximation with respect to d/ξ_n^* expression (17) takes on the form of (11) in the special case $\gamma_{B1}=\gamma_{B2}$.

It follows from the structure of the expression for κ (15) that the values of this parameter are confined to the range $1/\sqrt{2}\leqslant\kappa\leqslant1$, which permits the use of the following asymptotic forms of the elliptic functions in calculations with an adequate degree of accuracy when $1-\kappa^2\ll1$:

$$\operatorname{sn}(u)=\tanh u+\frac{1-\kappa^2}{4\cosh^2u}[\sinh u\cosh u-u],$$

$$\operatorname{cn}(u)=\frac{1}{\cosh u}+\frac{1-\kappa^2}{4\cosh^2u}\times[\sinh u\cosh u-u]\tanh u,$$

$$\operatorname{dn}(u)=\frac{1}{\cosh u}+\frac{1-\kappa^2}{4\cosh^2u}\times[\sinh u\cosh u-u]\tanh u.$$

In the zeroth approximation with respect to $1-\kappa^2$ the expressions found for the supercurrent [(2b) and (17)] asymptotically transform one into the other.

Plots of the temperature dependence of the critical current were calculated numerically for finite values of d/ξ_n^* and γ_B and are presented in Figs. 4 and 5. The points represent experimental data obtained in high-T_c SNS junctions with normal metal layers of noble metals. It is seen that there is satisfactory agreement between the experiment and the theoretical calculations.

3.4. Maximally asymmetric junctions ($\gamma_{B1}\ll\gamma_{B2}$)

In the limiting asymmetric case $\gamma_{B1}\ll\gamma_{B2}$ the spatial variation of the phases of the anomalous Green's functions in the N region is negligible in comparison with the spatial variation of their modulus F in a zeroth approximation with respect to γ_{B2}^{-1}. The coordinate dependence of F following from (3) and (4) is specified by expressions (13) and (15), in which γ_B and q should be replaced by γ_{B1} and $2q$, respectively. This result is natural, since at such large

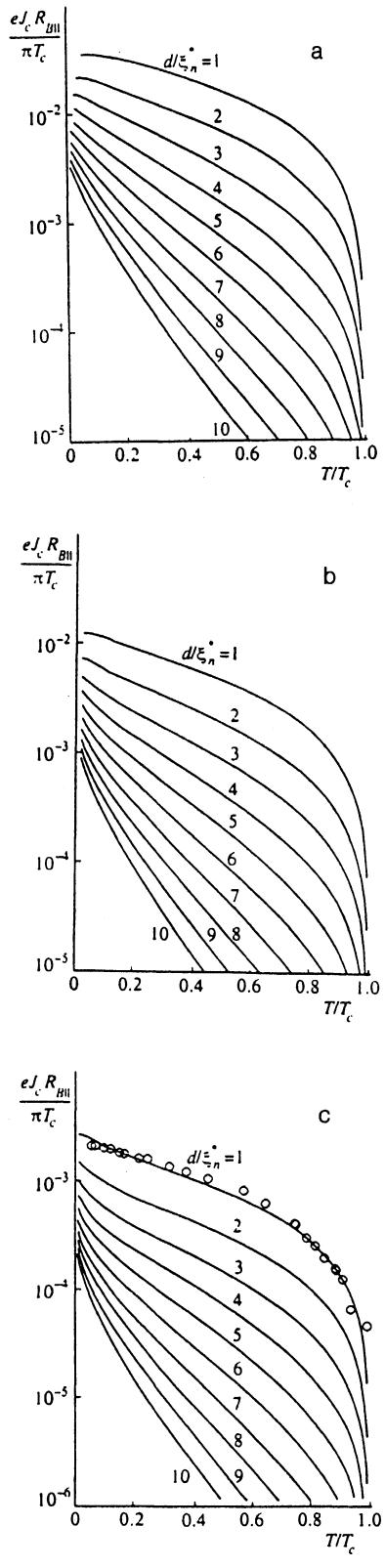

FIG. 4. Temperature dependence of the critical current of symmetric SNS structures ($\gamma_{B1}=\gamma_{B2}=\gamma_B$) calculated at fixed values of the suppression parameter $\gamma_B=10$ (a), 20 (b), 50 (c) and various N-layer thicknesses. The points represent experimental data.[13]

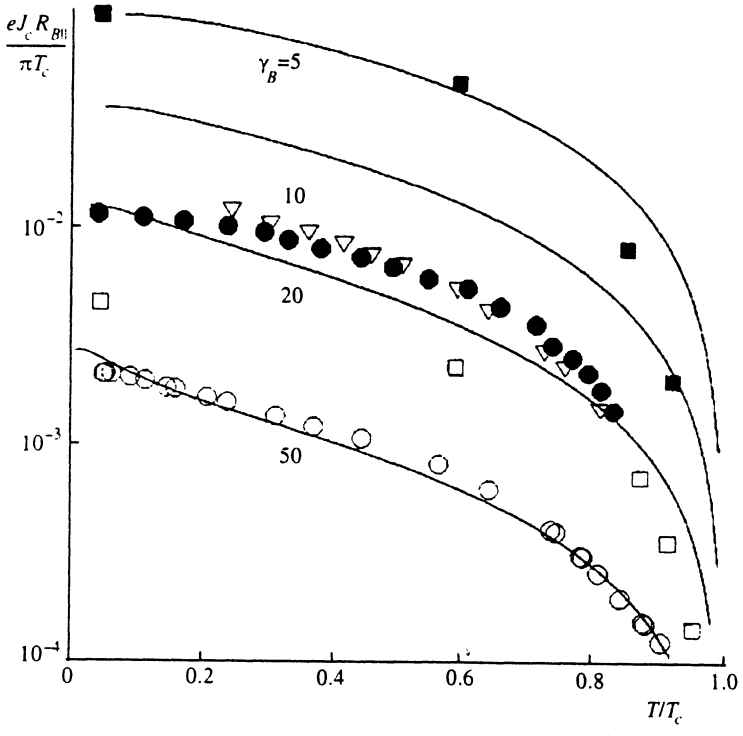

FIG. 5. Temperature dependence of the critical current of symmetric SNS structures ($\gamma_{B1}=\gamma_{B2}=\gamma_B$) calculated for $d/\xi_n^*=1$ and various values of the suppression parameter γ_B. The points represent experimental data from Refs. 10 (●), 3 (▽), 5 (□), and 13 (○).

values of γ_{B2} the superconducting properties in the normal metal layer of an SNS structure are determined only by the processes involving the diffusion of Cooper pairs through the boundary with the highest transparency and its stationary properties resemble the behavior of SINS junctions with an SN boundary of small transparency. In fact, in this approximation it follows from (2b) and (4) that

$$J_s=\frac{2\pi T}{e\rho_n\xi_n^*\gamma_{B2}}\sum_\omega\frac{\Delta F(-d/2)\sin(\varphi)}{\sqrt{[\omega^2+\Delta^2)(\omega^2+F^2(-d/2)]}}, \quad (18)$$

is specified by a formula similar to the known relation[22] for asymmetric SIS′ tunnel structures, in which the value of the modulus of the anomalous Green's functions in the normal metal on the interface having the smallest transparency is assigned by the equalities:

$$F\left(-\frac{d}{2}\right)=\omega\frac{2\kappa\sqrt{(1-\kappa^2)}}{1-2(1-\kappa^2)},$$

$$\kappa=\frac{\mathrm{dn}(q)}{\mathrm{cn}(q)}\sqrt{\frac{1}{2}+\frac{\Omega}{2\sqrt{(\Omega^2+\mathrm{Re}\,\Phi_s^2)}}},$$

$$q=\frac{d}{\xi_n^*}\sqrt{\frac{\omega}{2\pi T_c}}. \quad (19)$$

When $d\ll\xi_n^*$, expression (19) takes on the form of the previously known result for SINS junctions:[21]

$$F\left(-\frac{d}{2}\right)=\Delta\left[1+\frac{\gamma_B d}{\xi_n^*}\frac{\sqrt{(\omega^2+\Delta^2)}}{\pi T_c}\right]^{-1}. \quad (20)$$

The temperature dependence of the critical current for this case was calculated for arbitrary values of γ_B in Ref. 23.

4. NORMAL-STATE RESISTANCE OF AN SNS JUNCTION

To calculate the normal-state resistance of high-T_c SNS junctions, it is reasonable to assume that it is determined by the resistance of its boundaries, i.e., to neglect both the intrinsic resistance of its N material and the contribution to R_n appearing as a consequence of the partial conversion of the supercurrent into a normal current in the electrodes. Here it must be taken into account that as a consequence of the small transparency of the boundaries, the spatial distribution of the normal current differs significantly from the distribution of the supercurrent, so that all the boundaries in the structure make contributions to R_n. In symmetric planar junctions (see Fig. 1)

$$R_n=2\frac{R_{B\|}R_{B\perp}}{R_{B\|}+R_{B\perp}}, \quad R_{B\|}=\frac{\rho_n\xi_n^*}{W_n d_s}\gamma_{B\|}, \quad (21)$$

$$R_{B\perp}=\frac{\rho_n\xi_n^*}{W_s d_n}\left[\frac{2\gamma_{BM\perp}\xi_n^*}{L}+\sqrt{\gamma_{BM\perp}}\coth\frac{L}{\xi_n^*\sqrt{\gamma_{BM\perp}}}\right],$$

$$\gamma_{BM\perp}=\gamma_{B\perp}\frac{d_n}{\xi_n^*}, \quad (22)$$

where W_n is the width of the N film located between the electrodes, W_s is the width of the N film lying on the electrodes of the junction, L is its length in the x direction, and d_n and d_s are the thicknesses of the N and S films, respectively. Expression (22) was derived in Ref. 20 under the assumption $d_n\leqslant\gamma_{B\perp}\xi_n^*$, which holds in real experimental situations.

The total resistance of maximally asymmetric step-edge SNS structures (See Fig. 1b) is given by the expression

$$R_n=\frac{R_{B\parallel}R_{B\perp}}{R_{B\parallel}+R_{B\perp}}+R_{B\perp}, \tag{23}$$

in which, as in (21) and (22), $R_{B\parallel}$ and $R_{B\perp}$ are the resistances of the boundaries of structures (the surfaces of the S electrodes) oriented parallel and perpendicularly to the crystallographic c axis of the high-T_c superconducting films. It is noteworthy that, as follows from (22), there is a characteristic normal-current transfer length in the N film $L^*=\min\{L,\sqrt{d_n\xi_n^*\gamma_{B\perp}}\}$. When $L<L^*$, $R_{B\perp}$ is proportional to $\gamma_{B\perp}$. However, when L is large, self-restriction of further current transfer occurs and $R_{B\perp}\propto\sqrt{\gamma_{B\perp}}$.

5. CAUSES OF THE SUPPRESSION OF J_cR_n IN HIGH-T_c SNS JUNCTIONS

It follows from the foregoing calculations that there are three causes of the suppression of J_cR_n in high-T_c SNS junctions.

The first and principal cause is the small transparency of the SN boundaries in the structures. It follows from expressions (11), (17), and (18) for the critical current of such structures that $J_c\propto 1/\gamma_{B1}\gamma_{B2}$. The maximum value of the normal-state resistance [see (21) and (23)] $R_n\propto\max\{\gamma_{B1},\gamma_{B2}\}$. Therefore, their product

$$J_cR_n\propto\frac{1}{\min\{\gamma_{B1},\gamma_{B2}\}}$$

and is thus $\min\{\gamma_{B1},\gamma_{B2}\}$ times smaller than the characteristic voltage of "ideal" Josephson junctions.[1]

The second most important cause is the presence of an additional resistance shunting the junction. In fact, it follows from the foregoing calculations that in the general case the normal-state resistance of the structure R_n is smaller than the resistance $R_{B\parallel}$ of the portion of the junction along which both the normal current and the supercurrent flow. For example, when the geometric factors and the resistivities of the boundaries in symmetric junctions satisfy certain relationships, it follows from (21) that the shunting resistance $R_{sh}=R_{B\perp}$ may be significantly smaller than $R_{B\parallel}$, since

$$\frac{R_{sh}}{R_{B\parallel}}=\frac{W_sd_n}{W_nd_s}\left[\frac{\gamma_{B\perp}}{\gamma_{B\parallel}}\frac{d_n}{L}+\frac{1}{\gamma_{B\parallel}}\sqrt{\gamma_{B\perp}\frac{d_n}{\xi_n^*}}\right], \tag{24}$$

despite the existence of a strong inequality between the suppression parameters ($\gamma_{B\perp}\gg\gamma_{B\parallel}$).

According to (23), in maximally asymmetric junctions ($\gamma_{B\perp}\gg\gamma_{B\parallel}$) R_n is, in fact, determined by the resistivity of the least transparent boundary $R_{B\perp}$. However, a shunt naturally forms in this geometry, too, since the supercurrent is localized in a region of order ξ_{eff},[20] while the normal current transfers to a distance L^* in the N film, so that

$$\frac{R_{sh}}{R_n}\approx\frac{\xi_{\text{eff}}}{L^*}=\frac{\xi_{\text{eff}}}{\min\{L,\sqrt{\gamma_{B\perp}d_n\xi_n^*}\}},$$

$$\xi_{\text{eff}}=\xi_n^*\sqrt{\frac{\gamma_B\pi T_c}{\omega(\gamma_B+\pi T_c/\sqrt{\omega^2+\Delta^2})}}. \tag{25}$$

The third cause of the suppression of J_cR_n is the decrease in J_c as a consequence of the proximity effect of the parts of the N film which sustain and do not sustain the supercurrent. This mechanism is more important, the closer T is to T_c and the larger is the distance between the electrodes.

This factor is conveniently evaluated with the aid of the equation derived in Ref. 20

$$\Phi_n=\frac{G_s\Phi_s}{G_s+\gamma_B(\omega/\pi T_c)}+\xi_{\text{eff}}^2\frac{1}{G_n}(G_n^2\Phi_n')',$$

$$\xi_{\text{eff}}=\xi_n^*\sqrt{\frac{\gamma_B\pi T_c}{\omega(\gamma_B+\pi T_c/\sqrt{\omega^2+\Phi_s\Phi_s^*})}}, \tag{26}$$

which describes the superconducting properties induced in a thin film of a normal metal having a common boundary with a bulk superconductor characterized by γ_B. Taking into account that the modified Usadel functions appearing in (26) for the S electrodes $\Phi_s=\Delta$ and that in the case of greatest practical interest $d\approx\xi_n^*$ the sums over ω determining the supercurrent converge at

$$\omega\approx\Omega\approx\min\{\Delta_s/\gamma_B,\pi T_c(\xi_n^*/d_n)^2\},\quad T\ll T_c, \tag{27}$$

we see from (26) that $\xi_{\text{eff}}\approx\xi_n^*\sqrt{\pi T_c/\Omega}$ in the interesting limit of large values of the suppression parameter. In maximally asymmetric structures (see Fig. 1), we can use (26) and (27) to easily obtain the following estimates of the values of the functions Φ_n induced in the N region through the boundary with the highest transparency:

$$\Phi_n\approx\frac{\Delta G_s\pi T_c}{\gamma_B\omega}\alpha_1\alpha_2\frac{1}{\cosh(d/\xi_n^*)},\quad \alpha_1=\frac{d_s}{\xi_{\text{eff}}},$$

$$\alpha_2=\frac{d_n}{\xi_n^*\min\{\sqrt{T_c/T},d_n/\xi_n^*\}}. \tag{28}$$

Here $d=(h-d_s)/\cos\vartheta$ is the effective distance between the junction electrodes, d_s and d_n are the thicknesses of the S and N films, h is the height of the step in the substance, ϑ is its angle relative to the substrate, and $\alpha_1\leqslant 1$ and $\alpha_2\leqslant 1$ are additional suppression factors due to the mutual character of the proximity effect between individual parts of the N film.

6. CONCLUSIONS

It follows from the foregoing analysis that there are several factors which worsen the characteristics of high-T_c Josephson junctions and which must be taken into account in developing technologies for the fabrication of high-T_c Josephson strictures and in interpreting results obtained in them. Apart from the small transparency of the SN bound-

aries, they include the parasitic shunting of the junction and the mutual character of the proximity effect in the N film.

It is qualitatively clear that the presence of a normal shunt should negatively influence not only the absolute values of J_cR_n, but also the noise and signal characteristics of SQUID's based on such junctions.

In junctions of the planar type the formation of a shunt can be avoided by depositing a protective insulator layer on the surface of the high-T_c superconducting film before the step involving formation of the electrodes by electron lithography. In step-edge SNS junctions such a passivating layer can also be deposited by angled sputtering before sputter-deposition of the bridge film. However, ion etching of the parasitic part of the N film lying on the electrodes[14] is, in all likelihood, more effective.

In structures schematically represented by Fig. 1a the suppression of J_c as a consequence of the parasitic proximity effect in the normal metal layer is appreciable when the thickness of the N film is greater than or of the order of the thickness of the electrodes. In asymmetric step-edge junctions this mechanism [see (28)] can decrease J_c by several fold.

It should also be noted that the approach developed herein to the analysis of the processes in SNS junctions with SN boundaries of small transparency is applicable to the investigation of processes in low-temperature junctions with a layer of a doped semiconductor material.[14]

We thank A. I. Braginski, M. Bode, M. Siegel, U. Poppe, M. Faley, and O. V. Snigirev for some helpful discussions and for immediate access to their experimental data.

This research was supported by the Scientific Council for High-T_c Superconductivity, the Soros Foundation, and BMFT in the framework of grant BMFT-FKZ 13N 5924A.

[1] M. Yu. Kupriyanov and K. K. Likharev, Usp. Fiz. Nauk **160**, 49 (1990) [Sov. Phys. Usp. **33**, 340 (1990)].
[2] B. Schwartz, P. M. Mankiewich, R. E. Howard, L. D. Jackel, B. L. Straughn, E. G. Burkhart, and A. H. Dayem, IEEE Trans. Magn. **25**, 1298 (1989).
[3] M. G. Forrester, J. Talvacchio, J. R. Gavaler, M. Rooks, and J. Lindquist, IEEE Trans. Magn. **27**, 3098 (1991).
[4] M. S. Wire, R. W. Simon, J. A. Lnine *et al.*, IEEE Trans. Magn. **27**, 3106 (1991).
[5] M. S. Dilorio, S. Yoshizumi, K.-Y. Yang *et al.*, in Springer Proceedings in Physics, Vol. 64, Superconducting Devices and Their Applications, edited by H. Koch and H. Lübbig, Springer-Verlag, New York, 1992, pp. 120–126.
[6] M. S. Dilorio, S. Yoshizumi, K.-Y. Yang, J. Zhang, and M. Maung, Appl. Phys. Lett. **58**, 2552 (1991).
[7] M. A. M. Gijs, J. B. Giesbers, and F. C. M. J. M. van Delft, Appl. Phys. Lett. **59**, 1233 (1991).
[8] M. S. Dilorio, S. Yoshizumi, K.-Y. Yang, J. Zhang, M. Maung, and B. Power, in Advances in Superconductivity V Proceedings of the 5th International Symposium on Superconductivity, edited by Y. Bando and H. Yamauchi, Springer, Tokyo, 1993, p. 1161.
[9] R. H. Ono, J. A. Beall, M. W. Cromar *et al.*, Appl. Phys. Lett. **59**, 1126 (1991).
[10] P. A. Rosenthal, E. N. Grossman, R. H. Ono, and L. R. Vale, Appl. Phys. Lett. **63**, 1984 (1993).
[11] N. Missert, T. E. Harvey, R. H. Ono, and C. D. Reintsema, Appl. Phys. Lett. **63**, 1690 (1993).
[12] R. H. Ono, L. R. Vale, K. R. Kimmenau *et al.*, IEEE Trans. Appl. Superconductivity **3**, 2389 (1993).
[13] M. Bode, M. Siegel, and A. I. Braginski, Preprint, 1993; A. I. Braginski, in Abstracts of European Conference on Applied Superconductivity, Gottingen, Germany, 1993, p. 4.
[14] W. M. van Huffelen, T. M. Klapwijk, D. R. Heslinga, M. J. de Boer, and N. van der Post, Phys. Rev. B. **47**, 5170 (1993).
[15] M. Yu. Kupriyanov and K. K. Likharev, IEEE Trans. Magn. **27**, 2460 (1991).
[16] M. Yu. Kupriyanov, in Proceedings of the Conference of the Macroscopic Quantum Phenomena, Bratislava, 1992, p. 147.
[17] M. Yu. Kupriyanov, in Advances in Superconductivity V Proceedings of the 5th International Symposium on Superconductivity, edited by Y. Bando and H. Yamauchi, Springer, Tokyo, 1993, p. 1049.
[18] M. Yu. Kupriyanov and V. F. Lukichev, Zh. Eksp. Teor. Fiz. **94**, 139 (1988) [Sov. Phys. JETP **67**, 1163 (1988)].
[19] K. D. Usadel, Phys. Rev. Lett. **25**, 507 (1970).
[20] M. Yu. Kupriyanov, Sverkhprovodimost: Fiz., Khim., Tekh. **2**, 5 (1989).
[21] A. A. Golubov and M. Yu. Kupriyanov, Zh. Eksp. Teor. Fiz. **96**, 1420 (1989) [Sov. Phys. JETP **69**, 805 (1989)].
[22] I. O. Kulik and I. K. Yanson, The Josephson Effect in Superconducting Tunneling Structures, Nauka, Moscow, 1970 (Engl. transl., IPST, Jerusalem, 1972).
[23] A. A. Golubov and M. Yu. Kupriyanov, Phys. Lett. A **154**, 181 (1992).

Translated by P. Shelnitz